Testing high energy cosmic ray interaction models with the atmospheric muon data

L. G. Dedenko[ab]*, G. F. Fedorova[b], T. M. Roganova[b]
[a] *Faculty of Physics, Lomonosov Moscow State University*
Moscow 119991, Leninskie gory, Russia
[b] *Skobeltsyn Institute of Nuclear Physics, Lomonosov Moscow State University*
Moscow 119991, Leninskie gory, Russia

29.10.2014

Abstract

It has been shown that muon flux intensities calculated in terms of the SIBYLL 2.1, QGSJET II-04, and QGSJET 01 models in the energy range of 10^2–10^4 GeV exceed the data of the classical experiments L3+Cosmic, MACRO, and LVD on the spectra of atmospheric muons by a factor of 1.5 – 2. It has been concluded that these tested models overestimate the production of secondary particles with the highest energies in interaction of hadrons. The LHCf and TOTEM accelerator experiments show also some disagreements with these model predictions at highest energies of secondary particles.

1 Introduction

The longitudinal development of extensive air showers and, hence, the depth X_{max} of its maximum depends strongly on the rate of the projectile particle energy E fragmentation. If a probability of secondary particles production in the energy range of $\sim(\ 0.01\ -\ 0.6)E$ is high then the depth X_{max} is expected to be rather large. And contrary, in case of the severe energy fragmentation the length of a shower and the depth X_{max} of its maximum will be small.

The intensity of the muon flux in the atmosphere depends also on the secondary particles produced in this energy range of $\sim(0.01 - 0.6)E$. So, this energy interval is the most important for the extensive air shower longitudinal development. The study of the secondary particle production with the most highest energies is also of importance for understanding of hadronic interactions.

The extensive air shower data are interpreted in terms of some models of hadronic interactions. These models at the most highest energies of secondary particles are tested at the accelerator experiments LHCf [1] and TOTEM [2]. We suggest [3, 4, 5] to test also the most popular models of hadronic interactions with the atmospheric muon data [6, 7, 8], measured with rather high accuracy at energies above 10^2 GeV. This test is of the primary importance for the study of composition of the primary particles.

All features of the energy spectrum, arrival directions and a composition of the primary cosmic ray particles should be determined to understand the origin of cosmic rays, their possible sources and a transport of particles in various magnetic fields on their ways to the Earth.

In the standard approach the depth X_{max} of shower maximum as a function of energy E of the primary particle is used to study a composition. In the alternative approach the ratio α of signals $s_\mu(600)$ in the underground and $s(600)$ in the surface detectors at a distance of 600 m from the shower core is used to study the nature of the primary particles:

*e-mail: ddn@dec1.sinp.msu.ru

$$\alpha = s_\mu(600)/(s(600). \quad (1)$$

The Yakutsk array data interpreted in terms of the same model QGSJET II-03 [9] gave the heavy composition if no testing is applied and the light composition with testing [5]. The ratious α calculated in terms of the QGSJET II-03 model [9] for the primary protons (solid line) and the primary iron nuclei (dashed line) and the Yakutsk array data (points with the error bars) [10] are shown in figure 1 as functions of the signals $s(600)$ in the surface detectors when no testing is applied [3] and in figure 2 as functions of the energy E of the primary particle when testing was used [11].

It had been found [12] that the atmospheric muon energy spectrum calculated in terms of the QGSJET II-03 model [9] and with the ATIC-2 primary particle spectrum [13] is by a factor 1.5 lower than data [6, 7, 8]. In [12] the transport equations have been used to estimate the muon energy spectrum. Many other papers [14, 15, 16, 17] used the same method.

We suggest the very simple alternative method [11] to simulate the muon energy spectrum to test some hadronic interaction models.

2 Simulations

The package CORSIKA 7.4 [18] had been used to estimate the energy spectra $D(E_\mu)$ of muons in the energy range of 10^2 – 10^5 GeV in the atmosphere from the primary protons and helium nuclei with energies within the interval 10^2 – 10^7 Gev in terms of the QGSJET 01 [19], QGSJET II-04 [20], SIBYLL 2.1 [21] models with statistics 10^6 – 10^2 events.

To estimate these energy spectra of muons $D(E_\mu)$ with energies in the energy range of 10^2 – 10^5 GeV in the atmosphere we need to know

1) the energy spectra dI_p/dE and dI_{He}/dE of the primary protons and helium nuclei with energies within the interval 10^2 – 10^7 Gev;

2) at the level of observation the energy spectra of muons $S_p(E_\mu, E)$ and $S_{He}(E_\mu, E)$ produced in showers induced by the primary proton and helium nuclei with the fixed energies E in terms of the QGSJET 01 [19], QGSJET II-04 [20], SIBYLL 2.1[21] models.

Then the energy spectra of muons $D(E_\mu)$ are calculated as follows. The spectrum $D_p(E_\mu)$ in showers induced by the primary protons:

$$D_P(E_\mu) \cdot dE_\mu = \int dE \cdot (dI_P/dE) \cdot S_P(E_\mu, E) \cdot dE_\mu \quad (2)$$

The spectrum $D_{He}(E_\mu)$ in showers induced by the primary helium nuclei:

$$D_{He}(E_\mu) \cdot dE_\mu = \int dE \cdot (dI_{He}/dE) \cdot S_{He}(E_\mu, E) \cdot dE_\mu \quad (3)$$

The sum of these spectra at the level of observation:

$$D(E_\mu) = (D_p(E_\mu) + D_{He}(E_\mu)) \quad (4)$$

is the calculated spectrum of atmospheric muons. To estimate integrals (2) and (3) we have to calculate the spectra of muons $S_p(E_\mu, E) \cdot dE_\mu$ in showers induced by the primary protons with fixed energy E and the spectra of muons $S_{He}(E_\mu, E) \cdot dE_\mu$ in showers induced by the primary helium nuclei with fixed energy E in terms of various models for different values of energy E. Calculations have been carried out for 24 values of energy E for the primary protons and for 19 values of energy E for the primary helium neclei.

The energy spectra of muons $S_\mu(E_\mu, E)dE_\mu$ calculated in terms of for the model QGSJET II-04 [20] are shown in figure 3 for the primary protons with various fixed energies E (1 – $3.162 \cdot 10^2$, 2 – 10^3, 3 – 10^4, 4 – 10^5, 5 – 10^6, 6 – 10^7) GeV, and in figure 4 for the primary

helium nuclei with various fixed energies E (1 – 10^3, 2 – 10^4, 3 – 10^5, 4 – 10^6, 5 – 10^7 GeV). It should be noted, that dependence of these spectra on energy E_μ near the energy E of the primary particle is very sharp. The dependence of these spectra $S_\mu(E_\mu, E)dE_\mu$ on the model used is also of interest.

The muon spectra $S_\mu(E_\mu, E)dE_\mu$ calculated in terms of the various models (+ – SIBYLL 2.1 [21], □ – QGSJET II-04 [20], ∘ – QGSJET 01 [19]) are shown in figure 5 for the primary protons with the energy $E = 10^5$ GeV and in figure 6 for the primary helium nuclei with the energy $E = 10^5$ GeV.

To estimate integrals (2) and (3) we need also to know the primary particle energy spectra dI_p/dE and dI_{He}/dE. As the energy per nucleon is of importance only the energy spectra of the primary protons and helium nuclei should be taken into account.

At energies $E \leq E_1 = 3 \cdot 10^6$ GeV we have used Gaisser T. K. and Honda M. approximation [22] (GH) for the primary proton and helium nuclei:

$$dN_A/dE_k = K \cdot (E_k + bexp(c\sqrt{E_k})^\alpha, \tag{5}$$

where the parameters α, K, b and c are assumed as 2.74, 14900, 2.15 and 0.21, accordingly, for the primary protons ($A = 1$) and as 2.64, 600, 1.25 and 0.14, accordingly, for the primary helium nuclei ($A = 4$). We will use GH approximation as $(dI_p/dE)_{GH}$ and $(dI_{He}/dE)_{GH}$.

We suggested the modified GH approximation of the energy spectra of the primary particles at energies $E > E_1$. For the primary protons it looks as follows

$$(dI_p/dE)_m = (dI_p/dE)_{GH} \cdot (E_1/E)^{0.5}. \tag{6}$$

For the primary helium nuclei it should be as

$$(dI_{He}/dE)_m = (dI_{He}/dE)_{GH} \cdot (E_1/E)^{0.5}, \tag{7}$$

where $E_1 = 3 \cdot 10^6$ GeV.

Figures 7, 8, 9 show the energy spectra of the primary protons and the primary helium nuclei and of the sum of the primary proton and helium nuclei, respectively. At these figures the GH [22] and the modified Gaisser-Honda approximation (formulas (6) and (7)) are shown as dashed line. The various data are shown by different symbols: AMS02 [23] – solid line, ATIC-2 [13] – ∘, CREAM [24] – •, ARGO [25] – △, WCFTA [26] – ■, KASKADE (QGSJET II-03) [27] – × and KASKADE (SIBYLL2.1) [27] – +, RUNJOB [28] – □, TUNKA [29] – ♢ (all particles), SPHERE-2 [30] – ▲ (all particles).

The models QGSJET 01 [19], QGSJET II-04 [20], SIBYLL 2.1 [21] are tested with the help of the smooth approximation of the atmospheric muon data observed by the collaborations L3+Cosmic [6], MACRO [7] and LVD [8]. These muon data had been used for comparison with our results of simulations of the energy spectrum of muons.

3 Results and conclusion

The spectra of vertical muons $D_p(E_\mu)+D_{He}(E_\mu)$ in the energy range of 10^2 – 10^4 GeV calculated in terms of various hadron interaction models (SIBYLL 2.1 [21] (+), QGSJET II-04 [20] (□) and QGSJET 01 [19] (∘)) in showers induced by the primariy protons and helium nuclei are shown in figure 10. It can be seen that the SIBYLL 2.1 model [21] predicts the maximum intensity of the muon flux with the highest energies; the QGSJET 01 model [19] gives values which are smaller by approximately 30%. The QGSJET II-04 model [20] predicts an intermediate result. This conclusion is in agreement with the results shown in figure 3. Figure 10 also clearly demonstrates the steepening of the spectrum at energies of muons E_μ much higher than the decay constant $B_\pm$ of $\pi^\pm$ mesons in the atmosphere ($B_\pm \approx 100$ GeV). Comparison of the calculated spectra with experimental data allows testing models.

Figure 11 shows the ratio R of the muon energy spectrum $D(E_\mu)$ calculated in [12] in terms of the QGSJET II-03 model with the primary particle spectra [13] to results of our simulations in terms of the same model but for the GH spectrum [22] of the primary particles. The difference $\sim$ 20% may be accounted for the different primary spectrum used. Indeed, figures 7, 8, 9 demonstrate, that the ATIC-2 spectrum of the primary particles is (10 – 20)% above the GH spectrum used in our simulations. The smooth approximation of the results of the L3+Cosmic [6], MACRO [7] and LVD [8] experiments was taken as data for comparison.

The ratio of the spectra calculated in terms of various models to this approximation is shown in figure 12. It can be seen that this ratio in the muon energy range of 10^2 – 10^4 GeV increases from ~ 1.4 to ~ 1.6 for the SIBYLL 2.1 model [21], from ~ 1.3 to ~ 1.4 for the QGSJET II-04 model [20], and from ~ 1.2 to ~ 1.3 for the QGSJET 01 model [19]. The most important fact is that an increase in this ratio begins at energies $E_\mu > 10^3$ GeV and it reaches ~ 2 for the SIBYLL 2.1 model, $\sim$ 1.7 for the QGSJET II-04 model and ~ 1.55 for the QGSJET 01 model at $E_\mu = 10^4$ GeV. No slowing of this increase is observed at highest energies of muons. Thus, figure 12 demonstrates a very serious departure of the calculated spectra from the data reported in [6, 7, 8]. This difference is associated with a slower rate of fragmentation of the energy of incident particles in events of their interaction with nuclei in the atmosphere. Thus, these models overestimate the probability of the generation of secondary particles with the highest energies. According to the calculations, the main contribution to integrals (2) and (3) comes from secondary particles with energies in the ranges of $(0.01 - 0.6)E$ and $(0.001 - 0.1)\ E$, where E is the energy of an incident particle, for the primary protons and helium nuclei, respectively. This overestimated probability is also confirmed by the data of the LHCf [1] and TOTEM [2] accelerator experiments. For example, the QGSJET II-04 model [20] overestimates the density of charged particles $dN_{ch}/d\eta$ per unit of pseudorapidity at the pseudorapidity $\eta = 6.345$ by a factor of $k \approx 1.3$ as compared to the TOTEM data [2]. This difference increases at large η values because of the difference between the slopes of the calculated curve and the data from [2]. The QGSJET 01 [19] model predict the density $dN_{ch}/d\eta$ which is (18 – 30)% higher than that in [2], and the SIBYLL 2.1 model [21] gives the density which is (4 – 16)% lower in the interval $5.3 \leq \eta \leq 6.4$. However, the SIBYLL 2.1 model gives a significantly smoother dependence of the density $dN_{ch}/d\eta$. This dependence intersects the extrapolation curve of the data [2] at $\eta \sim 6.5$ and is significantly above this extrapolation curve at $\eta \sim 7$–8. Under the assumption of a similar dependence for charged mesons, this results in a decrease in the calculated density of muons at large distances x from the axis of the shower. This decrease was observed in the Pierre Auger Collaboration data [31] and Yakutsk EAS array data [32]. Comparison of the LHCf data [1] on the energy spectra of photons in p–p collisions at an energy of $\sqrt{s} = 7$ TeV with predictions of various models in the pseudorapidity range $8.81 \leq \eta \leq 8.99$ shows that the QGSJ II-03 model [9] gives a two to four times smaller number of photons, whereas the SIBYLL 2.1 [21] model predict a 1.5 – 2 times larger number of photons. Thus, all models should be significantly corrected for the highest energies of secondary particles.

4 Acknowledgements

Authors thank LSS (grant 3110.014.2) for support.

References

[1] O. Adrian, L. Bonech, M. Bongi (for the LHCf Collab.), Phys. Rev. **D 86**, 092001 (2012); H. Menjo, O. Adriani, and M. Bongi (for LHCf Collab.), Nucl. Instrum. Methods Phys. Res. **A 692**, 224 (2012).

[2] G. Latino (on behalf of TOTEM Collab.), arXiv: hep-ex/1302.2098v1 (2013).

[3] A. V. Glushkov, S. P. Knurenko, A. K. Makarov, I. T. Makarov, M. I. Pravdin, I. Ye. Sleptsov, L. G. Dedenko, T. M. Roganova, G. F. FedorovaA. V. Glushkov, A. Sabourov, in Proceedings of the 32th International Cosmic Ray Conference (Beijing, 2011) **1**, 213 (2011).

[4] L. G. Dedenko, S. P. Knurenko, A. K. Makarov, I. T. Makarov, M. I. Pravdin, I. Ye. Sleptsov, A. V. Glushkov, G. F. Fedorova, T. M. Roganova, and A. A. Sabourov, in Proceedings of the 33th International Cosmic Ray Conference (Rio-de-Janeiro, 2013); https:// 143.107.180.38/indico/contributionDisplay.py?contribId=0045&sessionId=3&confId=0

[5] L. G. Dedenko, G. F. Fedorova, T. M. Roganova, A. V. Glushkov, S. P. Knurenko, A. K. Makarov, I. T. Makarov, M. I. Pravdin, A. A. Sabourov and I. Ye. Sleptsov, J. Phys. G: Nucl. Part. Phys. **39**, 095202 (2012).

[6] The L3 Collab., arXiv: hep-ex/0408114v1K (2004).

[7] M. Ambrosio, R. Antolini, G. Auriemma et al. (The MACRO Collaboration), Phys. Rev. **D 52**, 3793 (1995).

[8] M. Aglietta, B. Alpat, E. D. Alieva et al. (The LVD Collaboration), arXiv: hep-ex/9806001v1 (1998).

[9] S. S. Ostapchenko, Phys. Rev. **D 74**, 014026 (2006).

[10] A. V. Glushkov, M. I. Pravdin, JETP **103**, 831 (2006).

[11] L. G. Dedenko, G. F. Fedorova, T. M. Roganova, A. V. Glushkov, S. P. Knurenko, A. K. Makarov, L. T. Makarov, M. I. Pravdin, A. A. Sabourov and I. Ye. Sleptsov, Journal of Physics: Conference Series **409**, 01 2068 (2013).

[12] A. A. Kochanov, T. S. Sinegovskaya, S. I. Sinegovsky, Astrop. Physics **30**, 219 (2008).

[13] A. D. Panov, J. H. Adams, Jr., and H. S. Ahn (for ATIC-2 Collab.), Bull. Russ. Acad. Sci.: Phys. **71**, 494 (2007); A. D. Panov, J. H. Adams, Jr., H. S. Ahn, et al., Bull. Russ. Acad. Sci.: Phys. **73**, 564 (2009).

[14] A. V. Butkevich, L. G. Dedenko, I. M. Zheleznykh, Soviet Journal of Nuclear Physics-Ussr **50**, 90 (1989).

[15] P. Lipari, Astropart. Phys. **1**, 195 (1993).

[16] E. V. Bugaev et al., Phys. Rev. **D 58**, 054001 (1998).

[17] L. V. Volkova, Bull. Russ. Acad. Sci. Phys. **71**, 560 (2007).

[18] D. Heck, J. Knapp, J.-N. Capdevielle G. Schatz, and T. Thouw, Forschungszentrum Karlsruhe Technical Report No. 6019, Karlsruhe (1998).

[19] N. N. Kalmykov, S. S. Ostapchenko, and A. I. Pavlov, Nucl. Phys. Proc. Suppl. **B 52**, 17 (1997).

[20] S. S. Ostapchenko, Phys. Rev. **D 83**, 014018 (2011).

[21] E.-J. Ahn, R. Engel, T. K. Gaisser, P. Lipari, and T. Stanev, Phys. Rev. **D 80**, 094003 (2009).

[22] T. Gaisser and M. Honda, Ann. Rev. Nucl. Part. Sci. **52**, 153 (2002).

[23] V. Choutko (on behalf AMS Collab.), in Proceedings of the 33th International Cosmic Ray Conference (Rio-de-Janeiro, 2013); https://143.107.180.38/indico/contributionDisplay.py?contribId=1262&sessionId=3&confId=0.

[24] H. S. Ahn (for the CREAM Collab.), Astrophys. J. Lett. **714**, L89 (2010).

[25] B. Bartoli (for the ARGO_YBJ Collab.), Phys. Rev. **D 85**, 092005 (2012).

[26] S. S. Zhang (for the WFCTA Collab.), Nucl. Instrum. Methods Phys. Res. **A 629**, 57 (2011).

[27] T. Antoni (for the KASCADE Collab.), Astropart. Phys. **24**, 1 (2005).

[28] V. A. Derbina, V. I. Galkin, and M. Hareyama (for the RUNJOB Collab.), Astrophys. J. **628**, L41 (2005).

[29] V. V. Prosin (on behalf TUNKA Collab.), in Proceedings of the 33th International Cosmic Ray Conference (Rio-de-Janeiro, 2013); https://143.107.180.38/ indico/contributionDisplay.py?contribId=0617&sessionId=3&confId=0.

[30] R. A. Antonov, T. V. Aulova, S. P. Beschapov, E. A. Bonvech, D. V. Chernov, T. A. Dzhatdoev, Mir. Finger, Mix. Finger, V. I. Galkin, N. V. Kabanova, A. S. Petkun, D. A. Podgrudkov, T. M. Roganova, S. B. Shaulov, and T. I. Sysoeva, in Proceedings of the 33th International Cosmic Ray Conference (Rio-de-Janeiro, 2013); https://143.107.180.38/indico/contributionDisplay.py?contribId=1185&sessionId=3&confId=0.

[31] R. Engel (for The Pierre Auger Collab.), arXiv: 0706.1921 [astro-ph] (2007).

[32] A. V. Glushkov, I. T. Makarov, M. I. Pravdin, I. E. Sleptsov, D. S. Gorbunov, G. I. Rubtsov, and S. I. Troitsky, JETP Lett. **87**, 190 (2008).

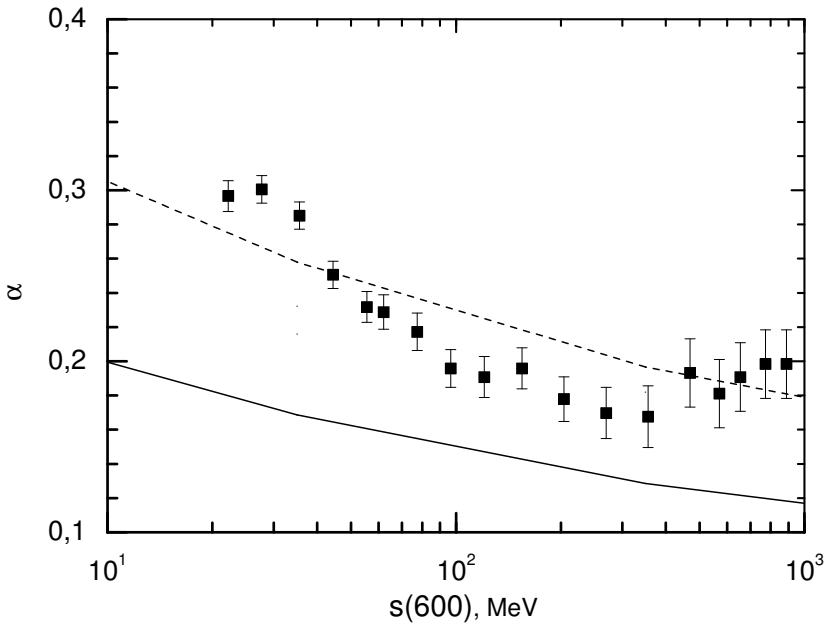

Figure 1: The fraction α of muons calculated in terms of the QGSJET II-03 model for the primary protons (solid line) and the primary iron nuclei (dashed line) and the Yakutsk array data [10] vs. the signal $s(600)$ in the surface detectors when no testing is applied.

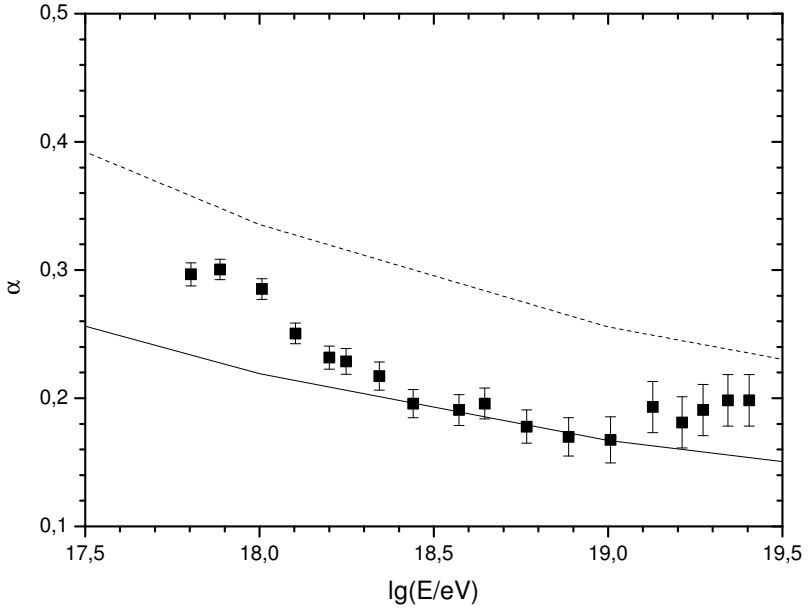

Figure 2: The fraction α of muons calculated in terms of the QGSJET II-03 model for the primary protons (solid line) and the primary iron nuclei (dashed line) vs. energy E of the primary particle when testing is applied.

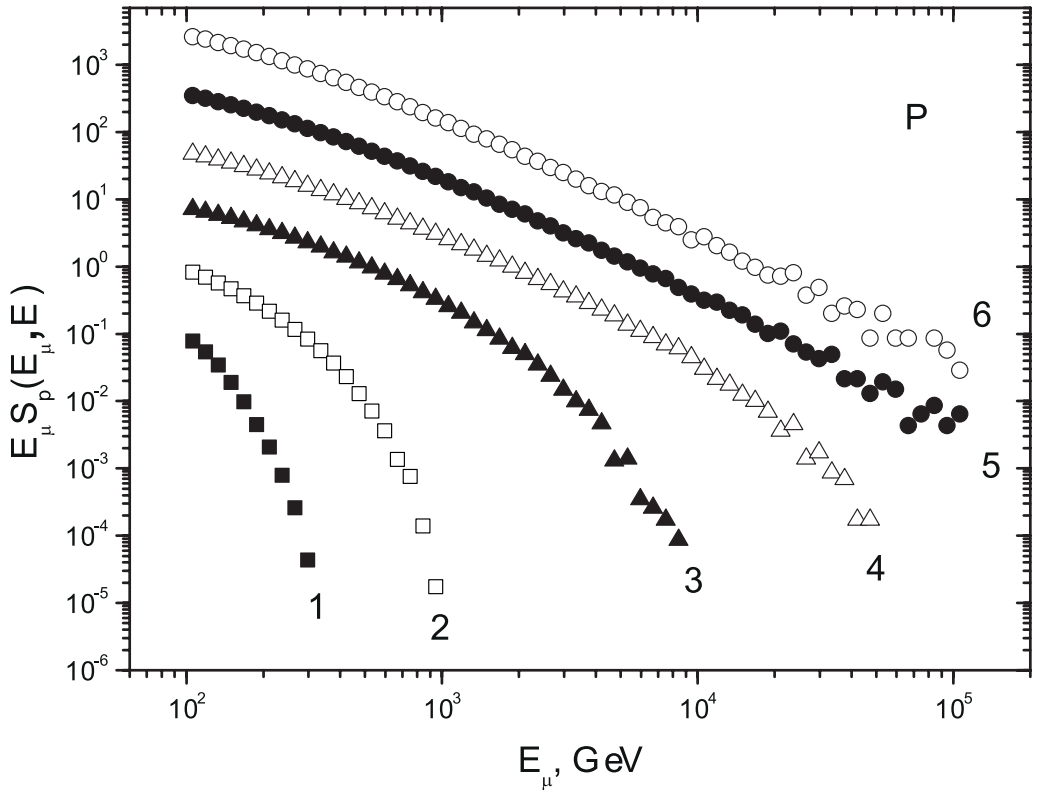

Figure 3: The energy spectra of muons generated in showers induced by the primary protons with various fixed energies E for the model QGSJET II-04: 1 – $3.162 \cdot 10^2$, 2 – 10^3, 3 – 10^4, 4 – 10^5, 5 – 10^6, 6 – 10^7 GeV.

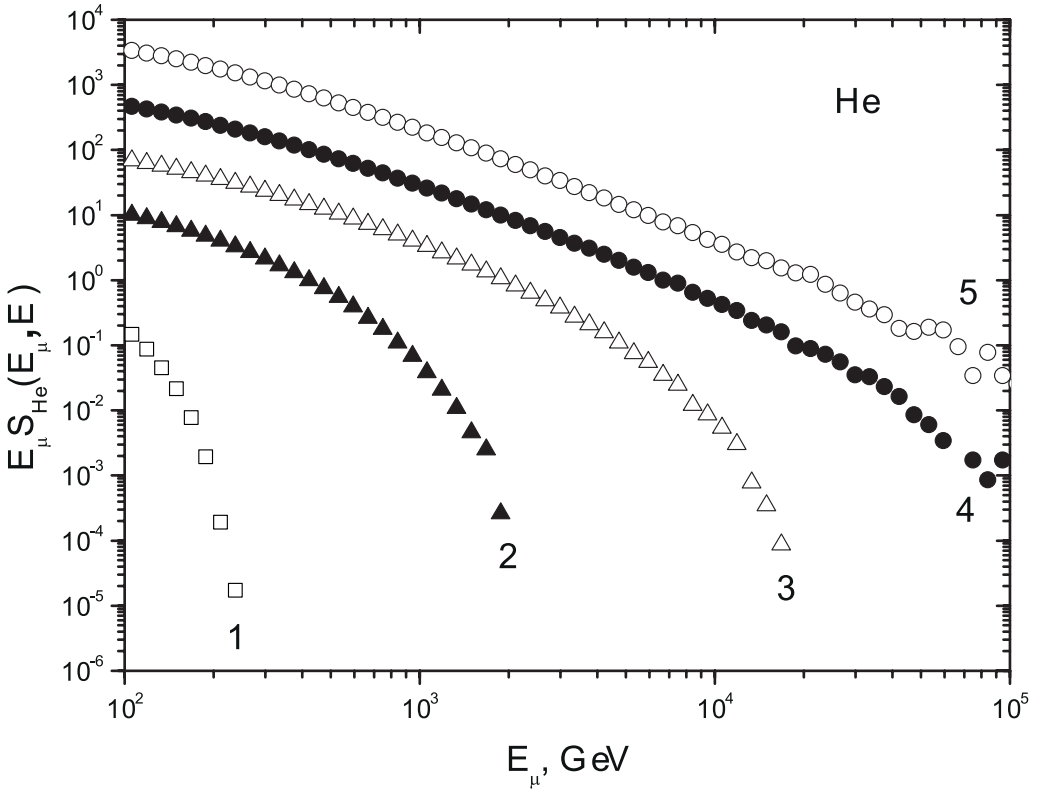

Figure 4: The energy spectra of muons generated in showers induced by the primary helium nuclei with various fixed energies E for the model QGSJET II-04: 1 – 10^3, 2 – 10^4, 3 – 10^5, 4 – 10^6, 5 – 10^7 GeV.

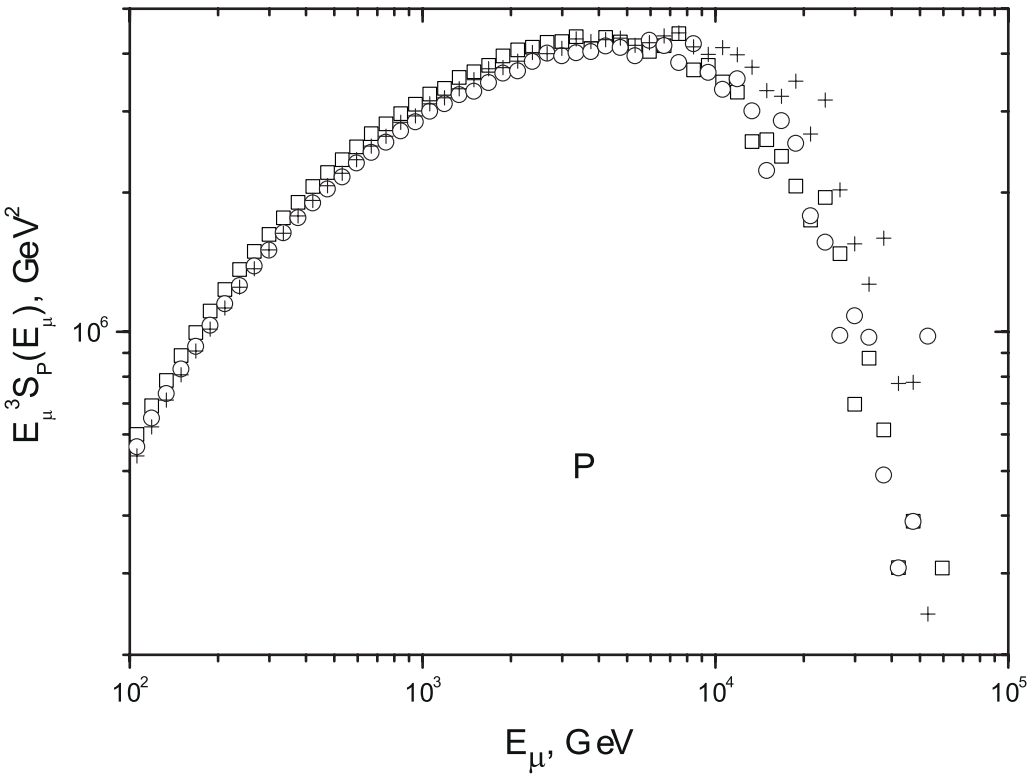

Figure 5: The muon energy spectrum calculated in terms of the various models: + – SIBYLL 2.1, □ – QGSJET II-04, ∘ – QGSJET 01 in showers induced by the primary protons with the energy $E = 10^5$ GeV .

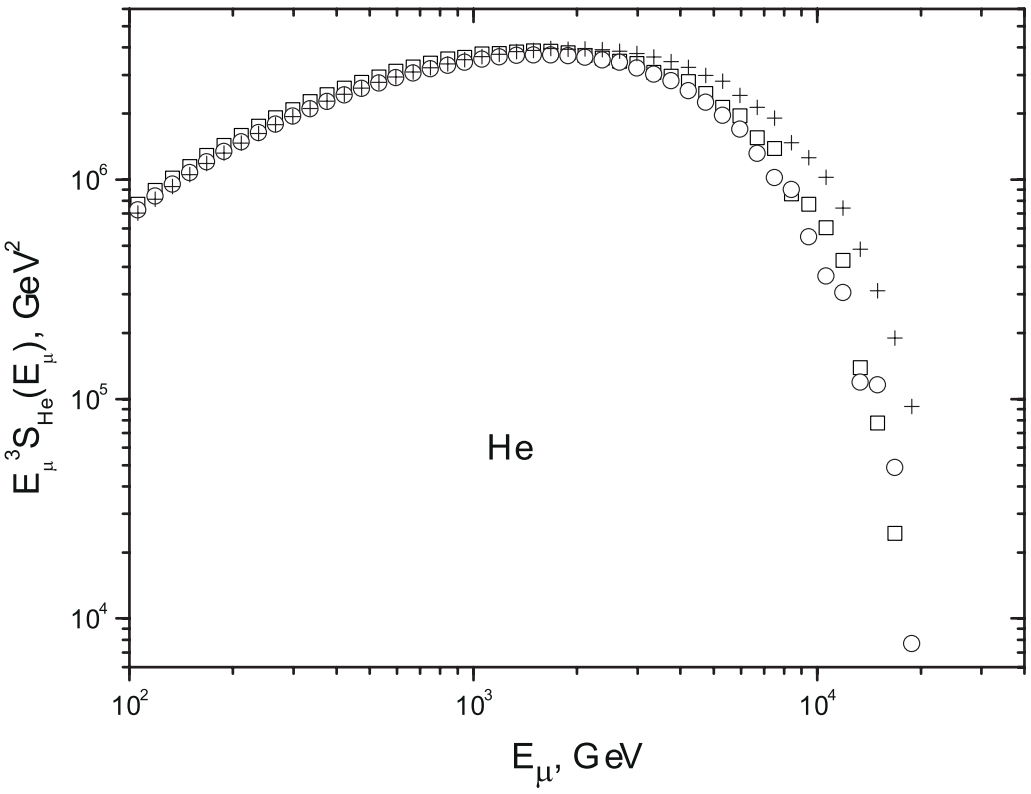

Figure 6: The muon energy spectrum calculated in terms of the various models: + – SIBYLL 2.1, □ – QGSJET II-04, ∘ – QGSJET 01 in showers induced by the primary helium nuclei with the energy $E = 10^5$ GeV .

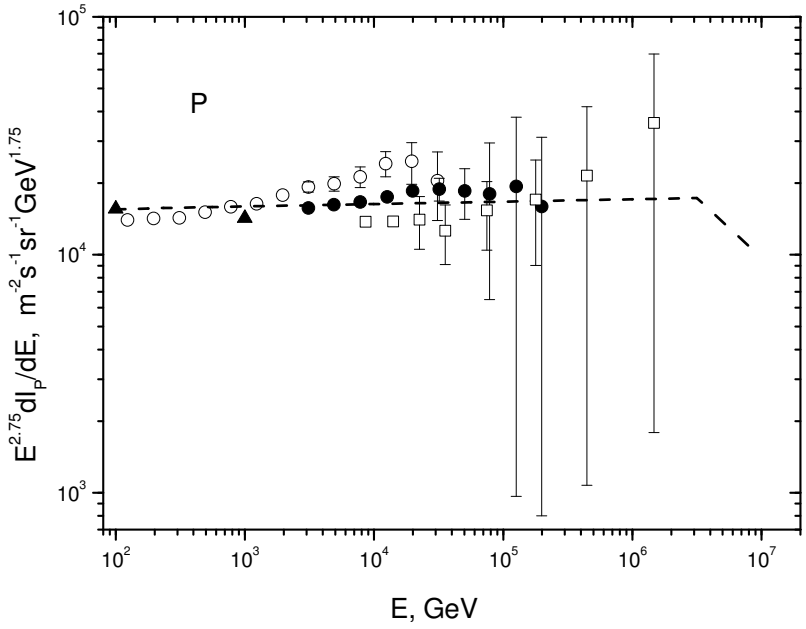

Figure 7: The energy spectrum of the primary protons.

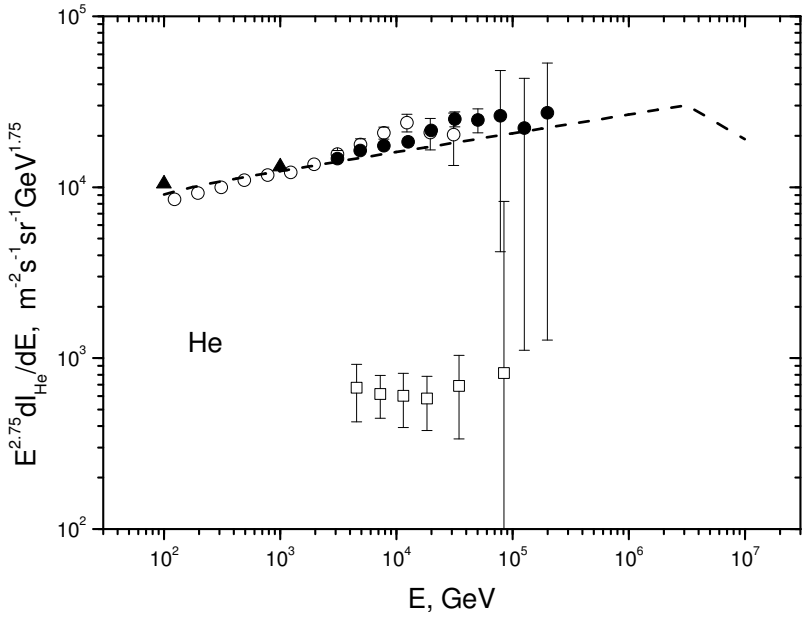

Figure 8: The energy spectrum of the primary helium nuclei.

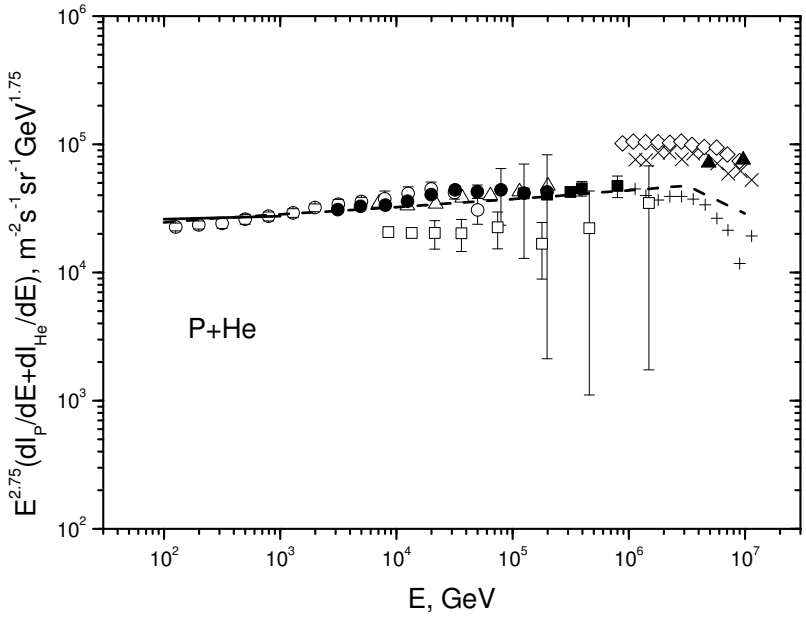

Figure 9: The sum of spectra of the primary protons and helium nuclei.

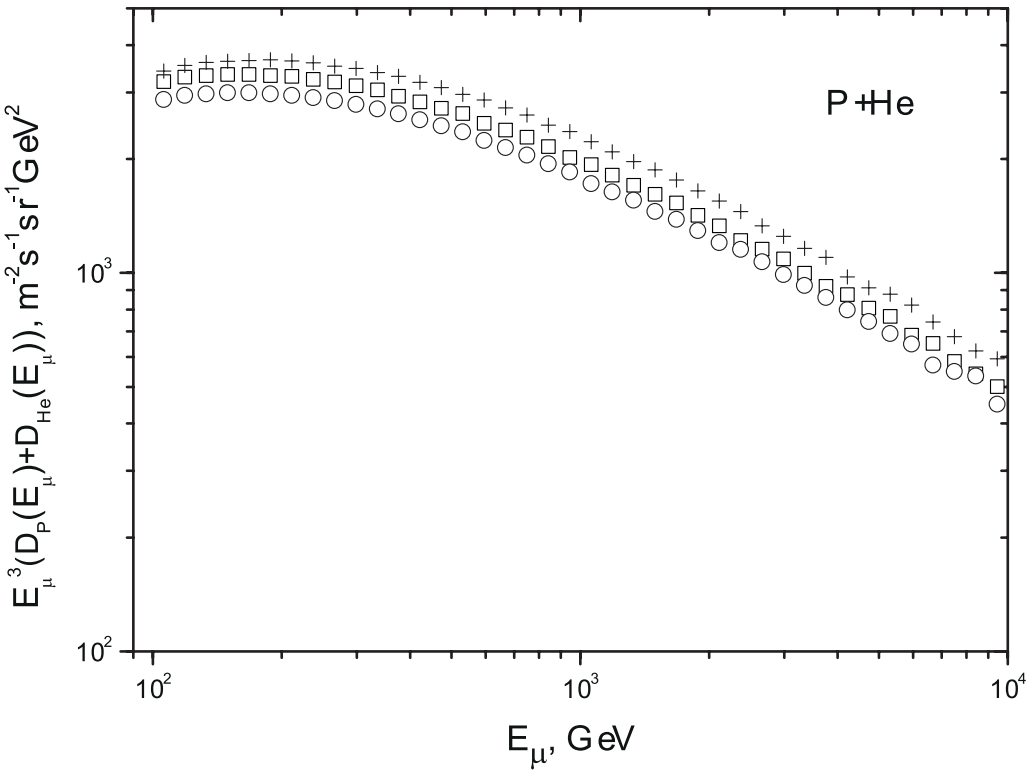

Figure 10: The atmospheric muon spectra simulated in terms of the SIBYLL 2.1 (+), QGSJET II-04 (□) and QGSJET 01 (○) models.

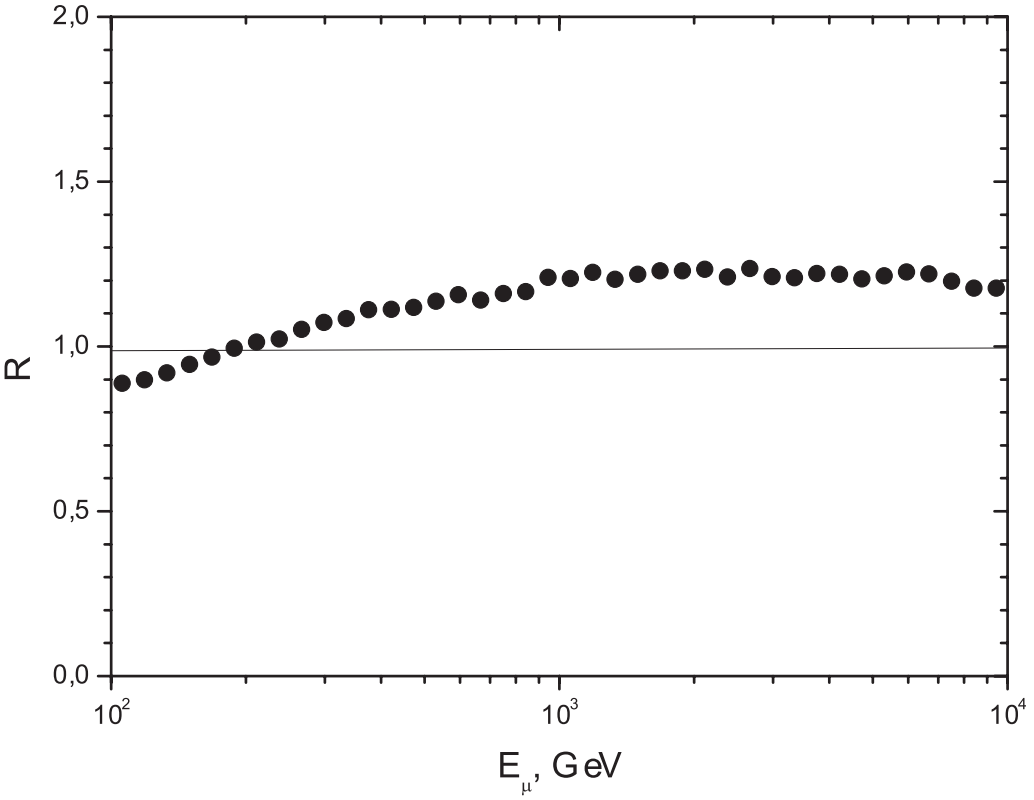

Figure 11: The ratious R of energy spectra of muons $D(E_\mu)$ calculated in [12] in terms of the model QGSJET II-03 to our spectra [11]

.

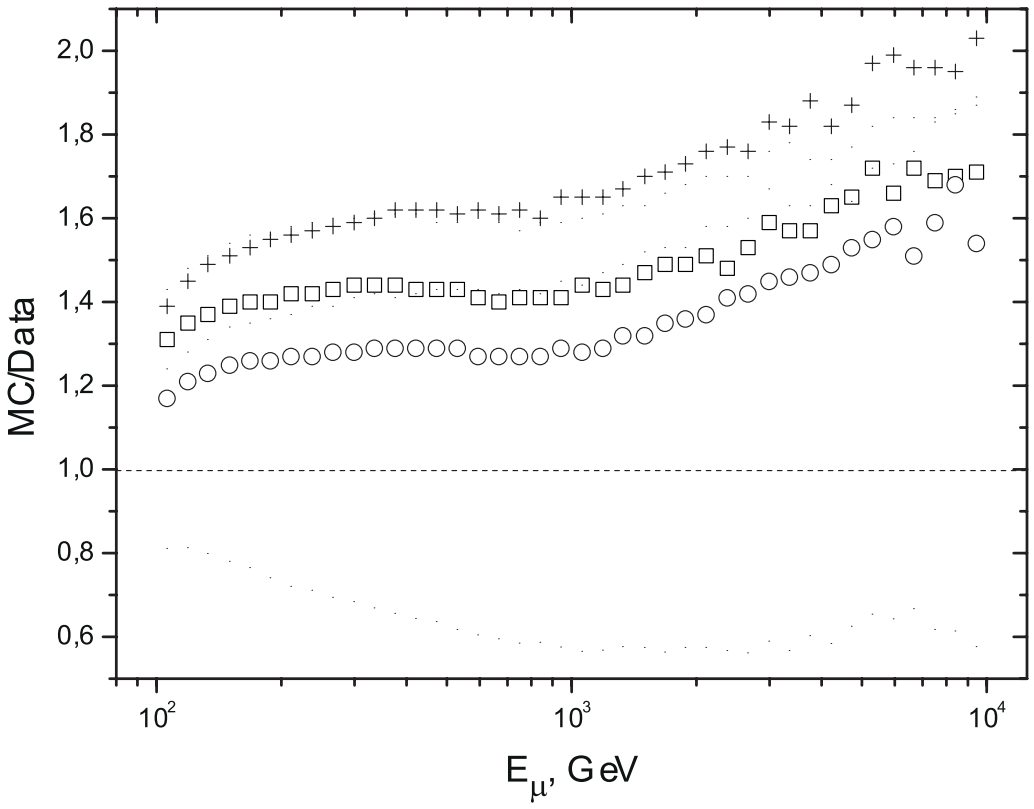

Figure 12: A comparison of calculated results with the atmospheric muon data [6, 7, 8] (MC/DATA): + – SIBYLL 2.1, □ – QGSJET II-04, ∘ – QGSJET 01.